doi: 10.4302/plp.2013.3.12 PHOTONICS LETTERS OF POLAND, VOL. 5 (3), 115-117 (2013)

Numerical Investigation of SPP Propagation at the Nano-scale MDM Waveguides with a Combiner

Md. Ghulam Saber,* Rakibul Hasan Sagor, Asif Al Noor, and Md. Thesun Al-Amin

Department of Electrical and Electronic Engineering, Islamic University of Technology, Gazipur, Bangladesh

Received February 01, 2013; accepted August 08, 2013; published September 30, 2013

Abstract—We present the propagation characteristics of Surface Plasmon Polariton in the nanoscale Metal-Dielectric-Metal waveguides which consist of a combiner. The propagation loss due to absorption by metal and reflection at the point of recombination is analyzed numerically. We have investigated the structure with different dielectric materials (air, aluminum gallium arsenide, gallium lanthanum sulfide) and for different wavelengths of the input signal. The wavelength dependent reflection coefficient, return loss and voltage standing wave ratio have also been reported in order to analyze the performance of the combiner.

Much interest has been focused on the research of Surface Plasmon Polariton (SPP) in the recent years [1] because of its extraordinary capability to travel through sub-wavelength sized holes. Besides, SPP can overcome the diffraction limit [2] which indicates the potential application in various fields such as biosensing [3], metamaterials [4], Bragg reflector [5], and efficient light coupling in solar cells [6]. However, efficient guiding of SPP is required in order to achieve compact integrated photonic devices. Several plasmonic waveguides have been proposed by the researchers in the past few years [7-9]. Among them, the Metal-Dielectric-Metal (MDM) structure has received much interest due to its ability to squeeze the SPP modes in the dielectric region. It can support sub-wavelength propagation mode from dc to visible [10] wavelength range.

Bends, splitters and recombination are inevitable parts of the optoelectronic devices. To our knowledge, several works on the analysis of SPP propagation in these shapes have been reported. G. Veronis *et al.* [11] showed that bends and splitters can be designed over a wide frequency range without much loss by keeping the centre layer thickness small compared to the wavelength. H. Gao *et al.* [12] investigated the propagation and combination of SPP in Y-shaped channels. B. Wang *et al.* [13] analysed two structures which consist of splitting and recombination.

In this paper, we investigate the SPP propagation characteristics in a 2D MDM waveguide with a combiner constructed with different dielectric materials [air, gallium lanthanum sulphide (GLS), aluminium gallium arsenide (AlGaAs)]. The characteristics that we have analyzed for the combiner are reflection coefficient, return loss and voltage standing wave ratio (VSWR). The propagation loss along the length of the waveguide is also reported. We expect that this study will provide a better understanding about the SPP propagation characteristics in an MDM waveguide with a combiner.

The simulation presented here is based on the Finite-Difference Time-Domain (FDTD) [14] method proposed by Yee. A general ADE-FDTD algorithm [15] is used to integrate the frequency dependent permittivity terms in the simulator.

We modelled the frequency dependent permittivity function of dielectric materials by a single pole Lorentz model which is given by,

$$\varepsilon_r(\omega) = \varepsilon_\infty + \frac{\omega_o^2(\varepsilon_s - \varepsilon_\infty)}{\omega_o^2 + j2\delta\omega - \omega^2}, \tag{1}$$

where: ε_∞ is the infinite frequency relative permittivity, ε_s is the zero frequency relative permittivity, j is the imaginary unit, δ is the damping co-efficient and ω_o is the frequency of the pole pair.

For modeling silver we used the six-pole Lorentz- Drude model which is as follows,

$$\varepsilon_r(\omega) = 1 - \frac{f_o\omega_p^2}{\omega^2 - j\Gamma_o\omega} + \sum_{i=1}^{5}\frac{f_i\omega_p^2}{\omega_{oi}^2 + j\Gamma_i\omega - \omega^2}, \tag{2}$$

where: ω_p is the plasma frequency, Γ_i is the damping frequency, f_i is the oscillator strength, and ω_{oi} is the resonant frequency.

The required parameters for simulation for different materials have been determined by many researchers. For silver we have used the parameter values obtained by Rakic *et al.* [16], for AlGaAs we have taken the values determined by M. Alsunaidi *et al.* [17] and for gallium lanthanum sulfide we have used the values determined by R.H. Sagor [18]. We take the step size as $\Delta x=\Delta y=5$nm, and the time step as $\Delta t = 0.95\cdot c^{-1}\cdot\left[\frac{1}{\Delta x^2}+\frac{1}{\Delta y^2}\right]^{-2}$, where c is the speed of light and taken as $c=3\cdot10^8\mathrm{ms}^{-1}$.

We set the mesh parameters FDTD algorithm accordingly in order to ensure the stability with minimum numerical dispersion.

* E-mail: gsaber@iut-dhaka.edu

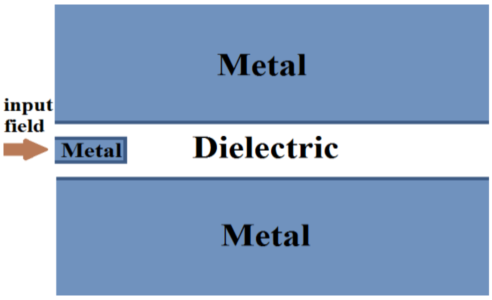

Fig. 1. Schematic Diagram of the MDM waveguide used for simulation.

The schematic diagram of the structure used for simulation is given in Fig. 1. The thickness of the dielectric layer before recombination is taken as 25nm for each section and after recombination as 70nm. The recombination occurs at a distance of 2.3µm.

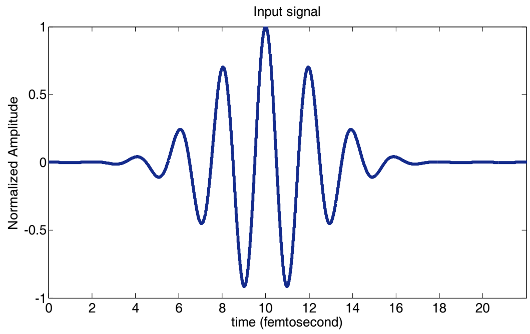

Fig. 2. The Normalized input signal in time domain.

At the beginning, we simulated the MDM waveguide with a recombination structure with the input pulse given in Fig. 2 in order to generate the SPP modes. Then we pumped the mode given in Fig. 3 into the structure modulated by a gaussian pulse having a characterisitc pulse width of 3 femtoseconds and different wavelengths.

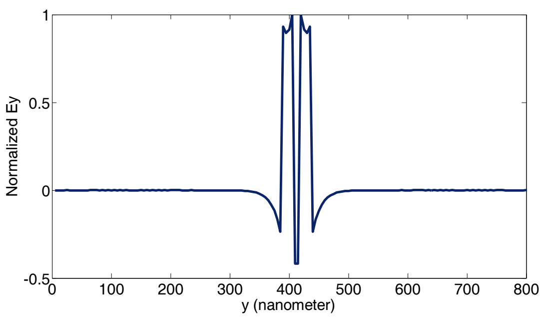

Fig. 3. The normalized Ey Profile pumped into the structure.

The reflection coefficient as a function of the wavelength has been determined numerically and presented in Fig. 4(i). From the figure it can be observed that the reflection coefficient is the highest at 600nm for air, 900nm for GLS and 1200nm for AlGaAs. At a telecom wavelength the reflection coefficient for air is the lowest having a value of 0.084 whereas for AlGaAs it is 0.863.

From the numerically determined reflection coefficient, we have obtained the return loss and VSWR using analytical equations the plot of which is given in Figs. 4(ii)-4(iii). At the optical communication wavelength the return loss for air is 21.5dB whereas for GLS it is 6.74dB and for AlGaAs it is 1.21dB.

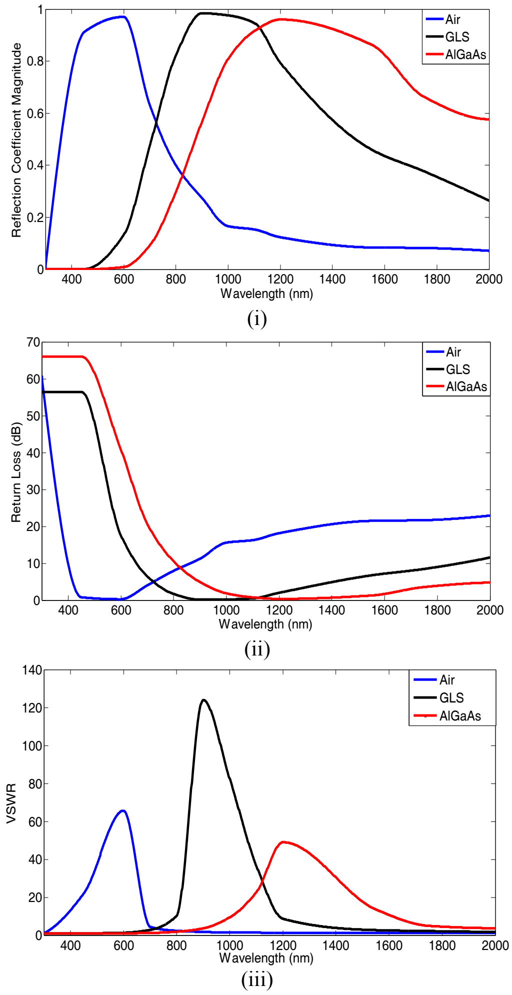

Fig 4. Numerically obtained (i) reflection coefficient (ii) return loss (iii) VSWR for the combiner for different materials as a function of wavelength.

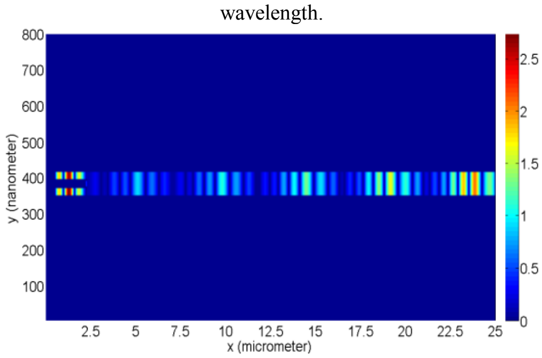

Fig. 5. Electric field distribution for the simulated MDM waveguide with the combiner.

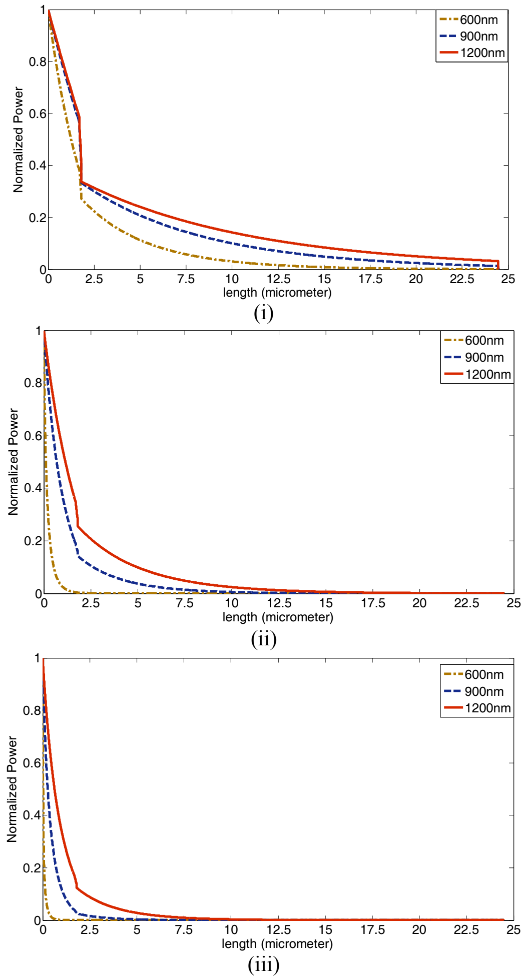

Fig. 6. Normalized Power Curve for (i) Air (ii) GLS (iii) AlGaAs.

The electric field distribution inside the waveguide after 74 femtoeconds is given in Fig. 5. The normalized power curve for different dielectric materials and different wavelengths of the input signal is also determined and presented in Figs. 6(i)-6(iii). From the figures, we can observe that there is a sharp fall in the power curve at 2.3μm, where the recombination occurs. This happens because of the discontinuity of the metal at the point of recombination. SPPs get scattered with multiple reflection at this point which causes a significant reduction of power.

The MDM waveguide constructed with air shows the least attenuation of power with distance, while the waveguide made by AlGaAs shows the highest attenuation. From the Figs. 6(i)-6(iii) we can also see that propagation loss depends on the wavelength of the input signal. When the wavelength is 600nm, the propagation length is about 12.5μm for air, 1.25μm for GLS and less than 1μm for AlGaAs, but when the wavelength is increased to 1200nm, the propagation length is extended to more than 25μm for air, 10μm for GLS and 5μm for AlGaAs.

The dispersion induced broadening of the input pulse is negligible for a propagation distance of 25μm in the materials that we have used. In order to observe this phenomenon we need to take propagation distances of, at least, 100μm for AlGaAs and more for the other two materials. However, due to the limitation of the resources we could not simulate the MDM waveguide with a combiner up to that propagation length.

We report the numerical analysis of SPP propagation in an MDM waveguide with a combiner. From our simulation we find that a sudden fall occurs in a normalized power curve at the point of recombination due to the back reflection of SPP. We also report the wavelength dependent nature of propagation length, reflection coefficient, return loss and VSWR. This analysis will be useful in the fabrication process of integrated photonic devices with combiners.

References

[1] T.W. Ebbesen, H. Lezec, H. Ghaemi, T. Thio, P. Wolff, Nature **391**, 667 (1998).

[2] D.K. Gramotnev, S.I. Bozhevolnyi, Nature Photon. **4**, 83 (2010).

[3] A. J. Haes , R.P. Van Duyne, J. Am. Chem. Soc. **124**, 10596 (2002).

[4] J. Henzie, M.H. Lee, T.W. Odom, Nature Nanotechn. **2**, 549 (2007).

[5] A. Hosseini, Y. Massoud, Opt. Expr. **14**, 11318 (2006).

[6] V.E. Ferry, L.A. Sweatlock, D. Pacifici, H.A. Atwater, Nano Lett. **8**, 4391 (2008).

[7] H. Ditlbacher, A. Hohenau, D. Wagner, U. Kreibig, M. Rogers, F. Hofer, F.R. Aussenegg, J.R. Krenn, Phys. Rev. Lett. **95**, 257403 (2005).

[8] W. Saj, T. Antosiewicz, J. Pniewski, T. Szoplik, Opto-Electr. Rev. **14**, 243(2006).

[9] G.S. Blaustein, M.I. Gozman, O. Samoylova, I.Y. Polishchuk, A.L. Burin, Opt. Expr. **15**, 17380 (2007).

[10] H. Shin, S. Fan, Phys. Rev. Lett. **96**, 73907 (2006).

[11] G. Veronis, S. Fan, Appl. Phys. Lett. **87**, 131102 (2005).

[12] H. Gao, H. Shi, C. Wang, C. Du, X. Luo, Q. Deng, Y. Lv, X. Lin, H. Yao, Opt. Expr. **13**, 10795 (2005).

[13] B. Wang, G.P. Wang, Opt. Lett. **29**, 1992 (2004).

[14] K. Yee, IEEE Trans. Antenn. Propag. **14**, 302 (1966).

[15] M.A. Alsunaidi, A.A. Al-Jabr, IEEE Photon. Technol. Lett. **21**, 817 (2009).

[16] A.D. Rakic, A.B. Djurišic, J.M. Elazar, M.L. Majewski, Appl. Opt. **37**, 5271 (1998).

[17] M. Alsunaidi, F. Al-Hajiri, Proc. PIERS, 1694 (2009).

[18] R.H. Sagor, Internat. J. Comp. Appl. **50**, 24 (2012).

